East Eur. J. Phys. **3**. 141-153 (2020) DOI:10.26565/2312-4334-2020-3-18

PACS: 87.14.C++c, 87.16.Dg

BINDING OF BENZANTHRONE DYE ABM TO INSULIN AMYLOID FIBRILS: MOLECULAR DOCKING AND MOLECULAR DYNAMICS SIMULATION STUDIES

Kateryna Vus
Department of Medical Physics and Biomedical Nanotechnologies, V.N. Karazin Kharkiv National University
4 Svobody Sq., Kharkiv, 61022, Ukraine
Corresponding Author: kateryna.vus@karazin.ua
Received 15 June 2020, revised June 29, 2020; accepted June 30, 2020

The binding of the benzanthrone dye ABM to the model amyloid fibrils of human insulin, referred to here as vealyl (12-VEALYL-17, insulin B-chain)), lyqlen (13-LYQLEN-18, insulin A-chain) and Insf (11-LVEALYL-17, B-chain) + 12-SLYQLENY-19, A-chain) was studied by the molecular docking and molecular dynamics simulations. To obtain the relaxed structures with the enhanced conformational stability, the model fibril structures were solvated and equilibrated in water at 300-310 K using the Gromacs simulation package, with backbone position restraints being applied to prevent the beta-sheet disruption. It appeared that the vealyl fibril relaxation resulted in the twisting of the two β-sheets, and only the vealyl fibril remained stable during 20 ns MD simulations of the relaxed structures. Next, Insf, vealyl, lyqlen, and vealyl (relaxed) fibrils were used for the molecular docking studies (by SwissDock), revealing the binding modes of ABM and standard amyloid marker Thioflavin T (ThT) to the examined fibril structures. Specifically, in the most energetically stable complex the vealyl (relaxed) fibril binding site for ABM was located on the dry steric zipper interface, although the dye was associated with only one twisted β-sheet. During the 20 ns MD simulation the ABM fibril location was changed to a deeper position in the dry interface between the two β-sheets, with the dye-interacting residues being represented by 6 LEU, 3 VAL, 2 ALA, 1 TYR and 1 GLU. The binging free energy ($\Delta G_{binding}$) for ABM complexation with vealyl (relaxed) fibril evaluated with the GMXPBSA GROMACS tool was found to be –31.4±1.8 kJ/mol, that is in accordance with our estimates derived from the fluorescence studies for ABM binding to the bovine insulin amyloid fibrils ($\Delta G_{binding}$ = –30.2 kJ/mol). The Lennard-Jones component appeared to dominate the dye-fibril interactions, with much smaller contributions of Coulombic and nonpolar solvation terms to the total $\Delta G_{binding}$ value, and unfavorable effect of the polar solvation term. These findings indicate that a high specificity of ABM to the insulin amyloid fibrils may arise predominantly from the dye-protein hydrophobic interactions, followed by the formation of van der Waals contacts, thus providing additional evidence for sensitivity of the dye spectral properties to environmental polarity, suggested in our previous studies. Overall, the obtained results provided further insights into the atomistic mechanism of the ABM binding to insulin amyloid fibrils and can be used for development of the novel fluorescent reporters possessing high sensitivity to the amyloid assemblies.
KEYWORDS: ABM, insulin amyloid fibrils, binding free energy, molecular docking, molecular dynamics simulations, Thioflavin T.

The formation of specific protein aggregates, amyloid fibrils, is currently associated with the development of severe human disorders, viz. Alzheimer's and Parkinson's diseases, systemic amyloidosis, etc. In view of this, detection and characterization of amyloid fibrils is very important for early medical diagnostics and testing the potential anti-amyloid drugs. Over the past decades, a great deal of effort has been invested in exploring the amyloid fibril formation at the atomistic level using the molecular dynamics simulations [1,2]. Along with elucidating the role of environmental factors (pH, temperature, ionic strength, etc.), increasing attention is paid to the interactions of amyloid fibrils with potential small molecule markers and inhibitors [3,4]. Insulin is a hormone, involved in the regulation of sugar level in blood, that contains 51 amino acids forming two polypeptide chains – A and B, connected by the disulfide bonds. Insulin pathological aggregation may result in the development of injection-localized amyloidosis in diabetic patients. Furthermore, the protein easily forms amyloid fibrils under acidic pH, increased temperature and ionic strength, resulting in the problems with the long-term storage of insulin pharmaceutical formulations. In our previous studies, we reported the applicability of the benzanthrone fluorescent dye, referred to here as ABM, to detection and characterization of the bovine insulin amyloid fibrils, with the advantages such as high quantum yield (*ca.* 0.52) and association constant (*ca.* 0.2 μM^{-1}) for the dye-protein complex, and a large shift (*ca.* 74 nm) of the dye emission maximum to the shorter wavelengths in the presence of fibrillized protein [5]. The aim of the present study is to obtain an atomistically detailed picture of the ABM binding to insulin amyloid species, using the molecular docking and MD simulations techniques, and to compare the ABM binding mode with that of the classical amyloid marker Thioflavin T [6]. Specifically, our goals were: i) to select from the database and to relax insulin amyloid fibril models (to enhance their stability) using the MD equilibration and the position restraints for the protein backbone and side chains; ii) to optimize the ABM/Thioflavin T structures and to calculate the atomic charges of the dye molecules (by RESP ESP charge Derive server) [7]; iii) to determine the ABM and ThT fibril binding modes by molecular docking (via SwissDock server [8,9]), using the unrelaxed and relaxed fibril structures; iv) to perform 20 ns MD simulations of the most energetically favorable dye-protein complexes and free proteins, in order to refine the stability of these complexes; v) to analyze the ABM-protein distances, protein RMSD, radius of gyration, position of the protein binding site for ABM/ThT, the dye effect on the fibril structure during MD simulations; vi) to estimate the binding free energy $\Delta G_{binding}$ of ABM/ThT to the fibrils and the impact of the Coulombic, Lennard-Jones, polar and nonpolar

© K. Vus, 2020

solvation components on the final $\Delta G_{binding}$ value using GMXPBSA GROMACS tool [10,11]; viii) to compare the theoretically predicted $\Delta G_{binding}$ values with those derived from the fluorescence studies and to reveal the predominant types of ABM interactions with the insulin fibrils.

MATERIALS AND METHODS

Preparation of the dye and insulin amyloid chemical structures

Four human insulin amyloid fibril models, referred to here as Insf, lyqlen, vealyl were used in this study. Insf, lyqlen and vealyl pdb structures were downloaded from the database provided by Sawaya M.R. [12–14]. Insf fibril is composed of 12 β-strands 11-LVEALYL-17 (insulin B-chain) and 12 β-strands 12-SLYQLENY-19 (insulin A-chain), forming two parallel in-register β-sheets. Lyqlen and vealyl fibril structures are composed of 12 β-strands 13-LYQLEN-18 (insulin A-chain) and 12-VEALYL-17 (insulin B-chain), respectively, forming two anti-parallel β-strands.

The relaxation of the amyloid fibrils was performed using the GROMACS software (version 2020.2) and CHARMM36-m force field, in order to enhance the conformational stability of the protein assemblies [15]. The input files for MD minimization and equilibration were prepared using the web-based platform CHARMM-GUI. The energy minimization (40 ps) of the lyqlen, vealyl, Insf structures was carried out in water (0.15 M NaCl for lyqlen, vealyl and neutralizing ions for Insf) using h-bond constraints (LINCS algorithm, lincs-order = 8) and the backbone restraints of 6 kcal/mol/Å^2 (5 kcal/mol/Å^2 for the Insf fibril).

MD equilibration of the lyqlen and vealyl amyloid species was performed in water, at 310 K, 0.15 M NaCl, using h-bond constraints (LINCS algorithm, lincs-order = 8). Simultaneously, position restraints for the side chains (0.1 kcal/mol/Å^2) coupled with backbone distance restraints of 6, 3.5, 2, 1.5, 1 kcal/mol/Å^2 descending steps with a total of 25 ns MD equilibration, followed by 10 ns equilibration without any restraints, were used. The resulting fibril structures are referred to here as vealyl (relaxed) and lyqlen (relaxed). The same h-bond constraints were employed for Insf MD equilibration in water, although it was carried out at 300 K in the presence of neutralizing ions, and using backbone distance restraints of 5, 2.5, 1, 0.5 kcal/mol/Å^2 descending steps with a total of 20 ns MD equilibration. The resulting Insf structure is referred to here as Insf (relaxed).

The .mol2 files of ABM and ThT were built in OpenBabelGUI, using the ligand structures drawn in MarvinSketch and optimized in Avogadro (.mrv files).

Molecular docking studies

The insulin fibril models (.pdb files): Insf, lyqlen, vealyl, vealyl (relaxed), and ABM, ThT (.mol2 files) structures were used for docking studies of the dye binding modes to the protein aggregates, performed by SwissDock web server [8,9]. SwissDock is based on EADock DSS software, that generates a huge number of ligand binding modes in the vicinity of all protein cavities (blind docking), followed by estimation the free energies of dye-protein binding in CHARMM22 force field. Next, ligand-protein complexes with the lowest binding energies are ranked, taking into account the solvent effect (implicit solvent model), clustered, and the most favorable clusters are included in the output-files of the docking studies. The performance of EADock DSS is good for the small and relatively rigid ligands, and for the cross-docking studies (when the protein structure does not present a perfect fit for the ligand) performance was about 40%, so the validation of the results is needed via, e.g. adding the flexibility to the protein [8,9].

The most energetically favorable dye-protein complexes were analyzed and visualized in the UCSF Chimera molecular viewer.

Molecular dynamics simulations of the insulin fibrils and the dye-fibril complexes

The 20 ns MD simulations were performed using the GROMACS package (version 2020.2) and the CHARMM36m force field. The input files for MD run of Insf (relaxed), lyqlen (relaxed) and vealyl (relaxed) fibril structures, as well as for the best energetically favorable ABM- and ThT-vealyl (relaxed) fibril complexes were prepared in CHARMM-GUI. The .itp files of ABM and ThT were constructed from the dye .mol2 files, using the CHARMM General Force Field, followed by replacing the ABM/ThT partial charges with those assigned by RESP ESP charge Derive Server [7]. The fibrils and dye-fibril complexes were solvated in a rectangular box with a minimum distance of 10 Å from the protein to the box edges and 0.15 M NaCl (neutralizing ions for Insf (relaxed) fibril) were added to the systems. The temperature was set at 310 K (300 K for the Insf (relaxed) fibril). The MD simulations were performed in the NPT ensemble. The minimization and equilibration of the dye-protein complexes were carried out during 5000 (10 ps) and 125000 (0.5 ns) steps, respectively. The constant temperature conditions were provided by the V-rescale thermostat. H-bonds were constrained using LINCS algorithm (lincs-order = 8). The molecular dynamics trajectories were corrected after the MD run, using the gmx trjconv GROMACS command and –pbc nojump option [10,11]. The commands gmx rms, gmx gyrate, gmx distance, gmx angle, and gmx make_ndx, included in GROMACS, were employed to calculate the protein backbone root-mean-square deviation ($RMSD$), protein radius of gyration (R_g), distances between the dye and protein centers of geometry, dihedral angles between benzanthrone and morpholine groups of ABM or between phenyl and benzothiazole

moieties of ThT, and to generate the index groups. Visualization of the snapshots of the MD runs and analysis of the protein secondary structures were performed in VMD.

Binding free energy calculations

The GMXPBSA 2.1 GROMACS tool allowing to post-process a series of representative snapshots from MD trajectories by combining explicit molecular mechanical energies and continuum (implicit) solvation models by MM/PBSA method, was used to calculate the binding free energies of a ABM-vealyl (relaxed) fibril complex [10,11]. This approach enables a rapid estimation of the free energy of binding ($\Delta G_{binding}$), exhibits a good correlation with experiment, although generally does not reproduce the absolute binding free energy values. The MM/PBSA method expresses the free energy of binding as the difference between the free energy of the complex ($G_{complex}$) and the sum of free energies of the protein ($G_{protein}$) and ligand (G_{ligand}):

$$\Delta G_{binding} = G_{complex} - \left(G_{protein} + G_{ligand}\right), \quad (1)$$

where $G_{complex}, G_{protein}, G_{ligand}$ are free energies of the ligand-protein complex, protein and ligand, respectively. The obtained difference is averaged over a number of trajectory snapshots.

The free energy terms for a ligand-protein complex, protein and ligand are calculated as averages of the thermodynamically weighted ensembles of structures obtained in MD simulations:

$$< G > = < E_{MM} > + < G_{solv} > - T < S_{MM} >, \quad (2)$$

$$E_{MM} = E_{int} + E_{coul} + E_{LJ}, \quad (3)$$

$$G_{solv} = G_{polar} + G_{nonpolar}, \quad (4)$$

where E_{int} comprises bond, angle and torsional angle energies; T is temperature (K); $< S_{MM} >$ is the entropic contribution of the solute; E_{coul}, E_{LJ} are the intramolecular Coulombic (electrostatic) and Lennard-Jones (van der Waals) energies, respectively; G_{solv} is the solvation free energy term, referring to the energy required to transfer the molecule from a continuum medium with a low dielectric constant (ε=1) to a continuum medium with the dielectric constant of water (ε=80); $G_{polar}, G_{nonpolar}$ are polar and nonpolar contributions to G_{solv}, respectively. The value of G_{polar} (the electrostatic contribution to the free energy of solvation, i.e. electrostatic free energy of the solute charge density optimized in electrolyte solution) was calculated using the linearized Poisson Boltzmann equation, and $G_{nonpolar}$ was considered to be proportional to the solvent accessible surface area ($SASA$) [16,17].

The binding free energy for ABM-vealyl (relaxed) fibril complex was calculated at every 100 ps from the 20 ns MD trajectory. Vealyl (relaxed) fibril and ABM topologies (.itp files) used for MD simulations were employed for the $\Delta G_{binding}$ calculations [10]. The term G_{solv} was calculated at 310 K, 0.15 NaCl using the APBS 1.4.1 suite. The E_{coul} and E_{LJ} contributions were determined using the GROMACS 2020.2 tools.

RESULTS AND DISCUSSION

The relaxation of amyloid fibrils with distance restraints has been suggested in previous MD simulation studies, because the available model structures of insulin fibrils appeared to be rather unstable in solution, that greatly complicates MD studies of the small-molecule-protein binding [15,18]. Insf, non-relaxed Insf, lyqlen and vealyl fibril structures are shown in Fig. 1A–C, while the relaxed ones are depicted in Fig.1D–F. The twisting of vealyl (relaxed) fibril (Fig. 1E) with respect to the long axis, made it different from the flattened pattern of the non-relaxed configuration (Fig. 1C). The increase in the vealyl (relaxed) curvature may be due to fibril tendency to minimize the electrostatic repulsion between the E13 residues of the β-sheets, as well as the unfavorable contacts of nonpolar amino acid residues with the solvent. Indeed, our previous studies of lysozyme, apolipoprotein A-I and Aβ amyloid fibrils in water under varying twisting angles, revealed the lowest fibril free energies for the angles *ca.* 15–20°, suggesting that the fibrils relaxed in solution are likely to prefer twisted configuration [19]. Further studies showed that 10 ns MD simulations of the solvated flattened lysozyme fibril configuration at 310 K did induce the increase of the fibril curvature [20].

It appeared that Insf (relaxed) and lyqlen (relaxed) structures were significantly destabilized (Fig. 1G,H), while the two β-sheets of the vealyl (relaxed) fibril remained twisted with respect to the fibril long axis, after 20 ns MD simulations

(Fig. 1I). Interestingly, high curvature of the vealyl (relaxed) fibril (Fig.1F) may enhance the fibril stability upon MD simulation (Fig.I), as compared to that of Insf and lyqlen (Fig.G,H). In turn, strong electrostatic repulsion within Insf, comprising the charged E13 (B-chain) and E17 (A-chain) residues, located closer to each other, than in lyqlen and vealyl, due to the parallel in-register β-strand orientation, may explain significant structural transformations of Inf upon relaxation (Fig.1D) and subsequent MD simulation (Fig.1G). Finally, lyqlen fibril tended to be planar after relaxation (Fig.1E) and MD simulation (Fig.1H) steps, presumably due to the higher elastic rigidity, as compared to that of vealyl [19]. However, some β-strands were detached from the lyqlen (relaxed) configuration (Fig.1H), suggesting that fibril stability may be increased upon restraining terminal β-strands during the MD simulations [18].

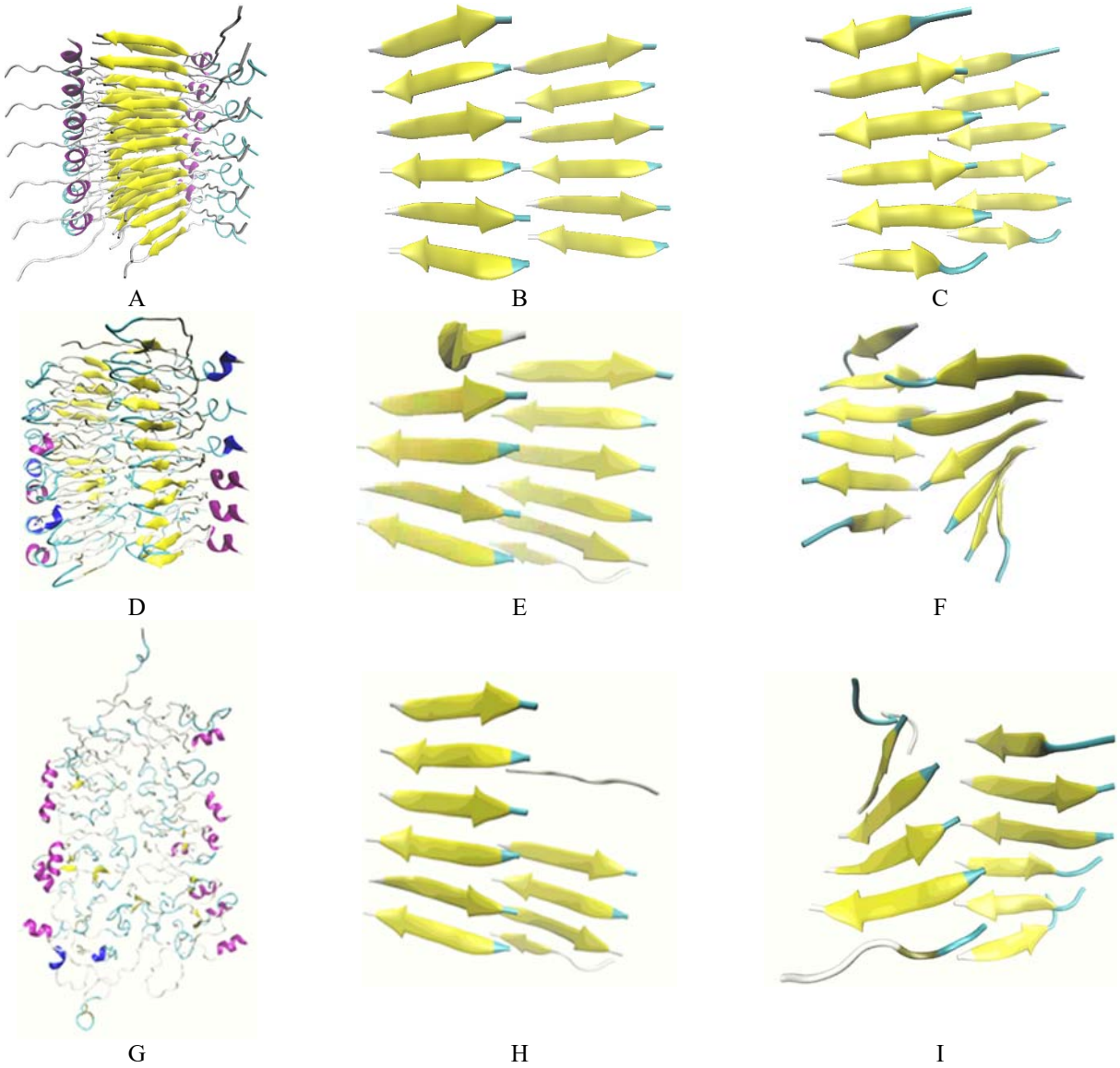

Figure 1. Insf (A), lyqlen (B) and vealyl (C) fibril structures downloaded from the websites: https://people.mbi.ucla.edu/sawaya/jmol/fibrilmodels; https://people.mbi.ucla.edu/sawaya/jmol/xtalpept/index.html. Snapshots of the 20 ns MD simulation of the insf (relaxed, D,G), lyqlen (relaxed, E,H), and vealyl (relaxed, F,I) fibrils relaxed in water. D,E,F – 0 ns, G,H,I – 20 ns. Protein structure is represented as NewCartoon. Protein is colored according to the secondary structure: yellow – extended β-sheets, cyan – β-turns, white – coil, magenta and blue – 310- and α-helices, respectively.

In view of the above, only the vealyl (relaxed) was used for further docking studies of the dye-protein binding, along with the non-relaxed Insf, lyqlen and vealyl fibrils. Shown in Figs. 2–6 are the most energetically favorable protein-ligand complexes (docking solutions), revealing the prevalent binding modes of ABM and ThT to the fibrils. For example, Fig. 2A represents all the ABM poses from the best 32 clusters, the most populated of which are located on the wet surface of the β-sheets almost perpendicular to the fibril long axis.

In the most stable ABM-Insf complex (Fig.2B) ABM interacts with 3 GLN residues of the A-chain β-sheet, as well as with 2 GLN, 1 PHE, 1 VAL and 1 HIS residues of the B-chain coil structure (these residues are located within the distance from the ABM molecule of ca. <5 Å). The free energy of the dye-protein binding ($\Delta G_{binding}$) calculated by

Swissdock was *ca.* –28.9 kJ/mol. Thus, ABM did not prefer to locate along the fibril channels, running parallel to the fibril long axis, as was suggested previously for lysozyme and insulin protein aggregates [5, 21,22]. However, docking results require further verification using the MD simulation of the complex combined with weak position restraints applied to all protein atoms [18].

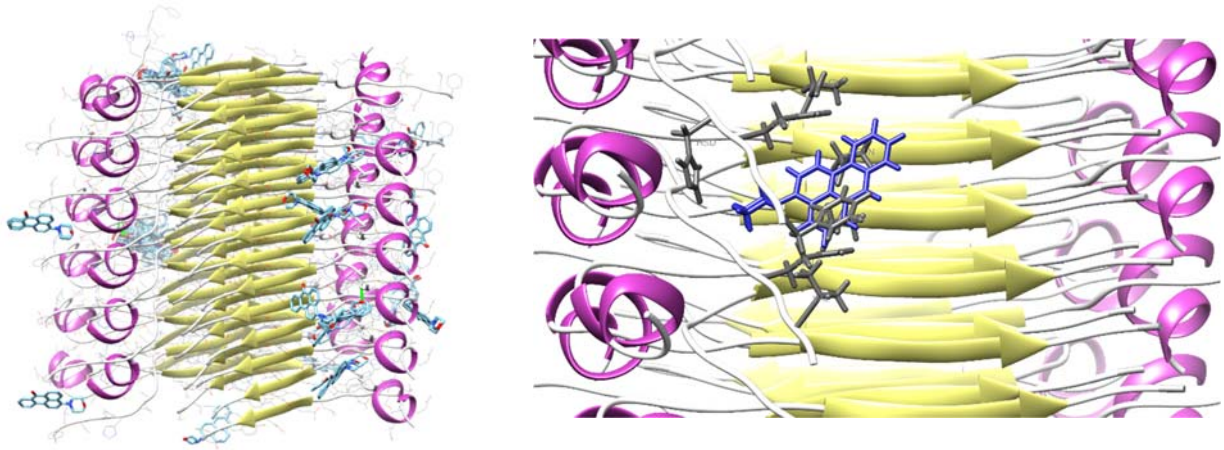

A B

Figure 2. The best docking (SwissDock) complexes between ABM and Insf amyloid fibril. A – All the dyes from 32 dye clusters, B – representative of the dye cluster (0.0) with the lowest $\Delta G_{binding}$ value (–28.9 kJ/mol). Protein and ABM structures are represented as NewCartoon/lines and sticks, respectively. The protein is colored according to the secondary structure: yellow – extended β-sheets, light grey – β-turns, white – coil. Dye molecules are colored by atom Name (C – cyan, O – red, N – blue), and the dye-protein hydrogen bonds are shown as green sticks (A). Insf residues, interacting with ABM, are represented as sticks and colored in dim grey (B).

Next, the best docking solutions for ABM-lyqlen and ABM-vealyl systems revealed the preferred dye location in the grooves L13_Q15/L16_ N18 (Fig. 3A) and L15_L17/ V12_A14 (Fig. 3B). Specifically, 5 LEU, 2 ASN, 1 GLN and 1 TYR16 lyqlen residues, or 2 ALA, 2 VAL, 4 LEU and 1 TYR16 vealyl residues were located in close vicinity of the fluorophore. ABM binds almost parallel to the lyqlen and vealyl long axes, although the clusters with the second largest population also revealed the dye association with the β-sheet edges (data not shown). Notably, $\Delta G_{binding}$ values for ABM complexation with lyqlen (–24.4 kJ/mol) and vealyl (–24.7 kJ/mol) were ~4 kcal/mol lower than that for ABM-Insf binding, most likely due to the greater separations of the dye from the fibril cores, resulting in the weaker van der Waals interactions.

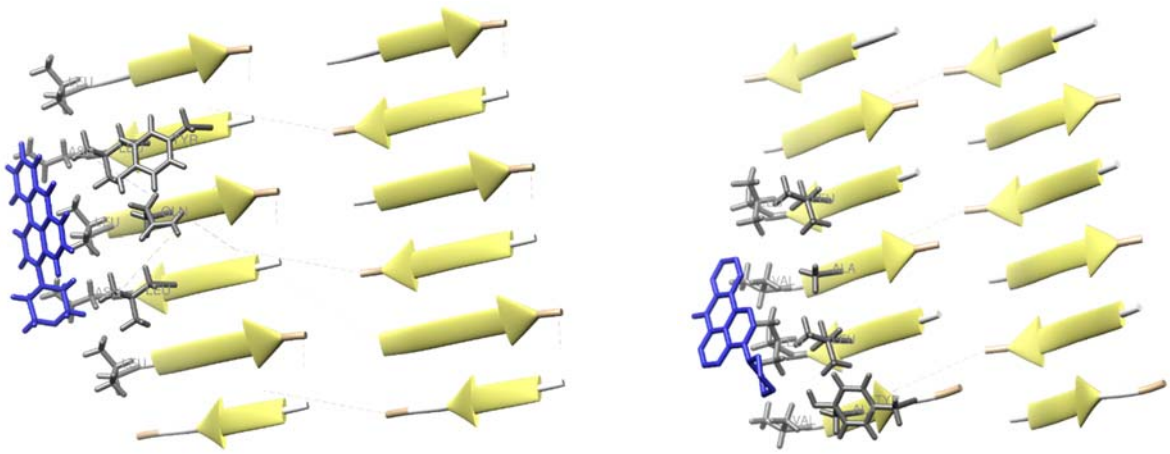

A B

Figure 3. The best docking (SwissDock) complexes between ABM and lyqlen (A) and vealyl (B) model fibrils. The lowest $\Delta G_{binding}$ values are –24.4 (A) and –24.7 (B) kJ/mol. The protein and ABM structures are represented as NewCartoon and sticks, respectively. Protein is colored according to the secondary structure: yellow – extended β-sheets, peach – β-turns, white – coil. Lyqlen/vealyl residues, interacting with ABM, are represented as sticks and colored in dim grey.

Fig. 4A represents the most stable ThT-Insf docking complex, possessing the lowest $\Delta G_{binding}$ value *ca.* –35.2 kJ/mol. ThT is attached parallel to the fibril long axis, to the groove L13_Q15 (4 LEU, 4 GLN residues of the A-chain), although the clusters in which the dye molecule binds to the β-sheet edges perpendicular to the fibril axis are largely populated (data not shown). In the most favorable binding mode (Fig. 4A), S-atom of ThT also forms intermolecular H-bond with the H-atom of the amide group of Q15, that may explain much greater $\Delta G_{binding}$ value as compared to that of ABM.

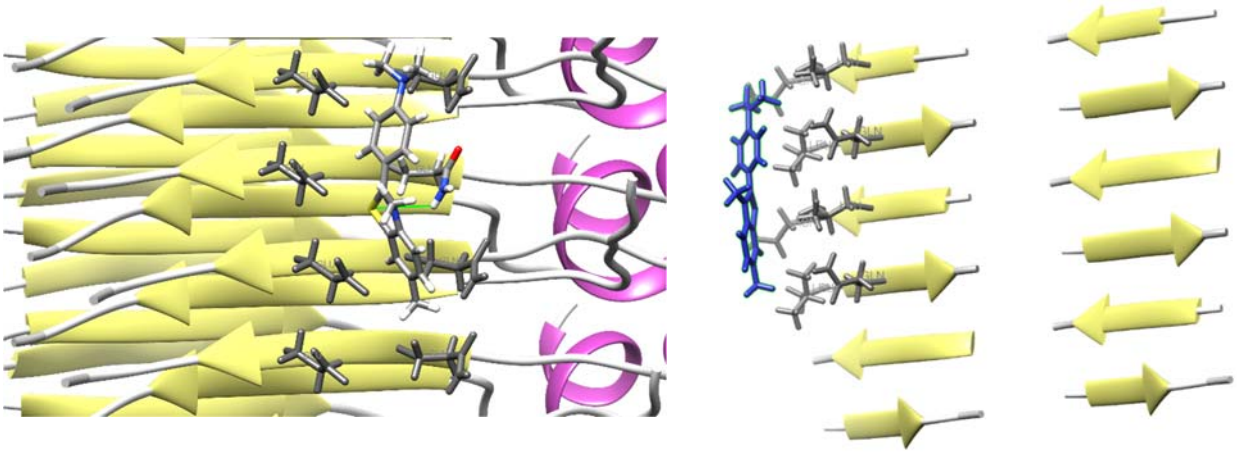

A B

Figure 4. The best docking (SwissDock) complexes between ThT and Insf (A) and lyqlen (B) amyloid fibrils. The lowest $\Delta G_{binding}$ values are –35.2 (A) and –25.5 (B) kJ/mol. The protein and ThT structures are represented as NewCartoon and sticks, respectively. The protein is colored according to the secondary structure: yellow – extended β-sheets, light grey – β-turns, white – coil. Dye molecules are colored by the atom name (C – dim grey, N – blue, S – yellow). Insf residues, interacting with ThT, are represented as sticks and colored in dim grey. The dye-protein hydrogen bond is shown as a green stick (A).

ThT also associated with the grooves L13_Q15/L16_N18 (4 LEU, 2 ASN, 2 GLN residues) of lyqlen (Fig. 4B) and L15_L17/V12_A14 (2 ALA, 2 VAL, 6 LEU residues forming the groove + 2 TYR16 residues outside of the groove) of vealyl (Fig. 5A) fibrils, although in several large clusters the dye also binds to the β-sheet edges perpendicular to the fibril axis (data not shown).

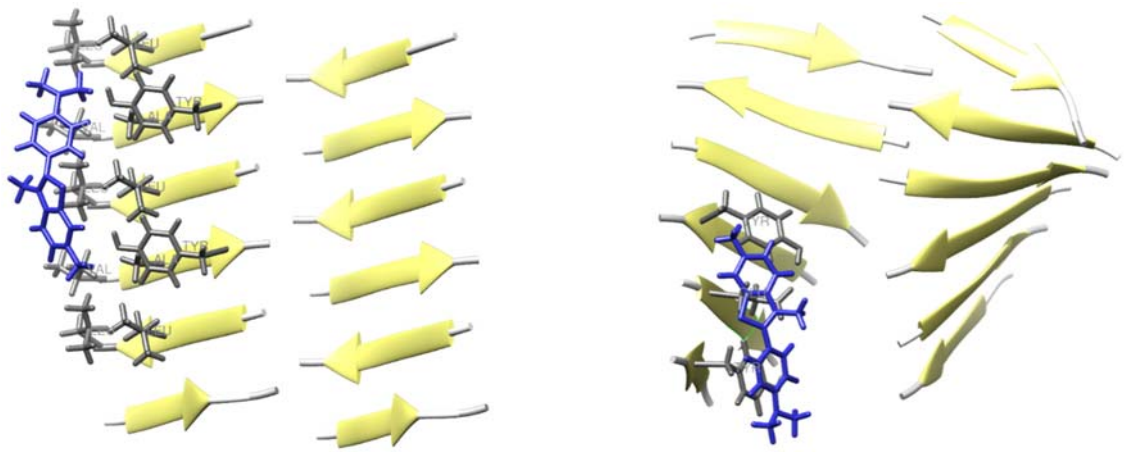

A B

Figure 5. The best docking (SwissDock) complexes between ThT and vealyl (A) and vealyl (relaxed) (B) amyloid fibrils. $\Delta G_{binding}$ values are –25.3 (A) and –28.2 (B) kJ/mol. The protein and ThT structures are represented as NewCartoon and sticks, respectively. The protein is colored according to the secondary structure: yellow – extended β-sheets, light grey – β-turns, white – coil. Vealyl residues, interacting with ThT, are represented as sticks and colored in dim grey.

In the latter case, S atom of ThT forms the H-bonds with C_a atoms of LEU16/ASN18 lyqlen and with the N-termini of LEU15/TYR16/LEU17 vealyl residues, while N2 atom of ThT forms the H-bonds with GLN15/GLU17 lyqlen and with the N-terminus of ALA14 vealyl residues. The $\Delta G_{binding}$ values for ThT-lyqlen and ThT-vealyl complexation were estimated to be *ca.* –25.5 and –25.3 kJ/mol, respectively, that is about 10 kJ/mol lower than the corresponding value for

ThT-InsF binding, presumably due to the absence of the dye-protein H-bonds and a more remote ThT location relative to the lyqlen and vealyl fibril cores. The above data validated the commonly recognized ThT-fibril binding mode for the studied insulin fibril structures [6]. Furthermore, half of the protein residues representing Insf, lyqlen and vealyl binding sites for the dye were represented by LEU, that is in good agreement with the studies of Biancalana and coworkers, who revealed a high affinity of ThT for TYR/LEU cross-strand ladders [23].

By analogy with the approach of Amdursky et al., who studied the interactions of photoacids with insulin amyloid fibril surfaces, using the Insf fibril model, the docking of ThT and ABM was also performed with vealyl (relaxed) fibril model. The best ThT-vealyl (relaxed) complex was characterized by the dye binding to the part of the β-sheet (2 TYR16, 1 GLU13 residues) parallel to the fibril axis (Figs. 5B,6A).

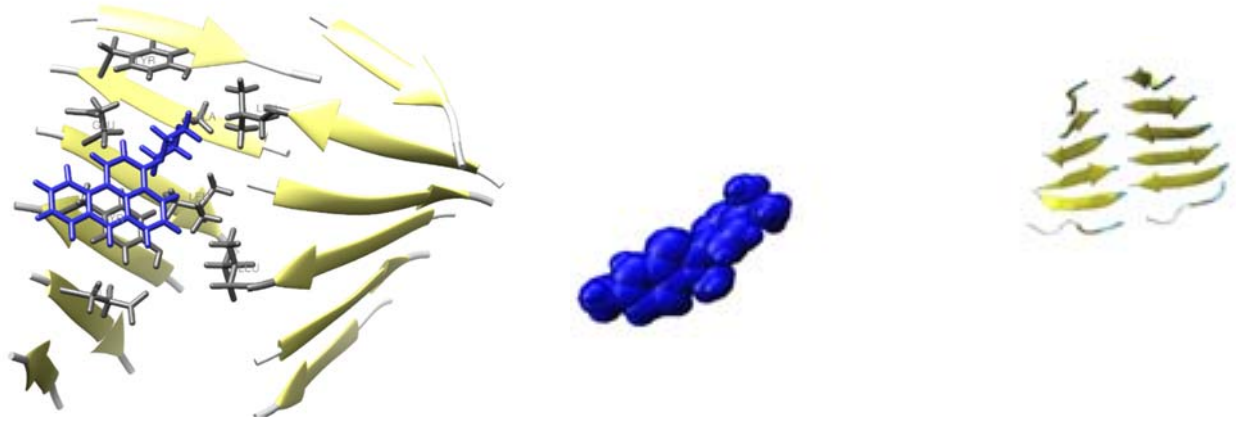

A B

Figure 6. A – The best docking (SwissDock) complex between ABM and vealyl (relaxed) amyloid fibril with $\Delta G_{binding}$ value –27.2 kJ/mol. The protein and ABM structures are represented as NewCartoon and sticks, respectively. The protein is colored according to the secondary structure: yellow – extended β-sheets, light grey – β-turns, white – coil. The vealyl residues interacting with ABM are represented as sticks and colored in dim grey. B – the last frame (20 ns) of the MD simulation of the best docking complex between ThT and vealyl (relaxed) amyloid fibril. The protein and ThT structures are represented as NewCartoon and VDW, respectively. The protein is colored according to the secondary structure: yellow – extended β-sheets, cyan – β-turns, white – coil.

The ThT formed few contacts with vealyl (relaxed), in contrast to vealyl, most likely due to the low affinity for the twisted fibril structures. Indeed, the dye did not bind to the highly twisted β-sheets of globular proteins [3]. Furthermore, in our previous molecular docking studies of the ThT interactions with the model twisted lysozyme fibrils, ThT preferred to locate in the central channels of the fibrillar assemblies, where the twisting angles are minimal, and the binding free energy values decreased with increasing the curvature of fibrillar aggregates [20]. Notably, 10 ns MD simulation of the solvated ThT-flattened lysozyme fibril complex at 310 K resulted in the fibril twisting, accompanied by the dye moving from the specific binding site (fibril channel) to the β-sheet edge [20].

Surprisingly, the most stable ThT-vealyl (relaxed) complex had $\Delta G_{binding}$ value *ca.* –28.2 kJ/mol, that is about 3 kJ/mol greater than that for the ThT-vealyl complex, where more amino acid residues are located in close vicinity of the dye. Such discrepancies may occur due to the smaller ThT distance from the vealyl (relaxed) core, resulting in the stronger van der Waals intermolecular interactions.

Fig.6A represents the best docking solution for ABM-vealyl (relaxed) binding, revealing that the dye is attached along the twisted fibril axis and interacts with 2 TYR, 3 LEU, 2 GLU, 1 ALA residues of the dry "steric zipper interface", although the ligand molecule may also be aligned perpendicular to the fibril axis and attached to the β-sheet surface and to the β-sheet edges (data not shown). $\Delta G_{binding}$ value for the ABM-vealyl (relaxed) complex was equal to –27.2 kJ/mol, that is about 2 kJ/mol greater than that for the ABM-vealyl one (Fig.3B), presumably due to stronger van der Waals contacts formed between the dye and the residues of the two β-sheets (Fig.6A).

In order to validate the stability of the docked ABM-vealyl (relaxed) and ThT-vealyl (relaxed) complexes, the 20 ns molecular dynamics simulations were performed at 310 K, 0.15 M NaCl, which is long enough for the binding site residues to relax, followed by the calculations of the ABM-fibril binding affinity [18]. It appeared that ThT was completely detached from the vealyl (relaxed) binding site (Fig. 6B), similar to the ThT-lysozyme fibril complex [20]. Thus, investigation of the ThT-fibril interactions should be performed using the flattened insulin amyloid fibril models, and position restraints could be applied to the terminal β-strands in order to increase stability of the fibril structures [18]. Notably, more dynamically stable molecular docking solutions for the ThT-vealyl (relaxed) complex can be obtained through using the ThT .mol2 file with the corrected charges on atoms calculated by RESP ESP charge Derive server.

In contrast to ThT, ABM showed a higher affinity for vealyl (relaxed) fibril, because it remained attached to the protein during 20 ns MD simulation (Fig.7), although the dye molecule was relocated from the initial fibril binding site

and was buried deeper into the dry interface between the two β-sheets (Fig.7D,E). Additional evidence for the change of ABM binding mode is provided by the time evolution of the dye-protein distance (Fig.8A): first, the distance increased from ~0.85 to ~1.15 nm, followed by a significant drop to a final value of *ca.* 0.55 nm, starting from about 6 ns of the MD simulation. The last frame (20 ns, Fig.7D,E) revealed that in the novel fibril binding site ABM axis is almost perpendicular to the fibril axis, and 6 LEU, 3 VAL, 2 ALA, 1 TYR and 1 GLU residues are located in close vicinity of the dye. The increased number of contacts formed between ABM molecule and vealyl (relaxed) confirms the stabilization of the final ABM-fibril complex (Fig. 7D,E).

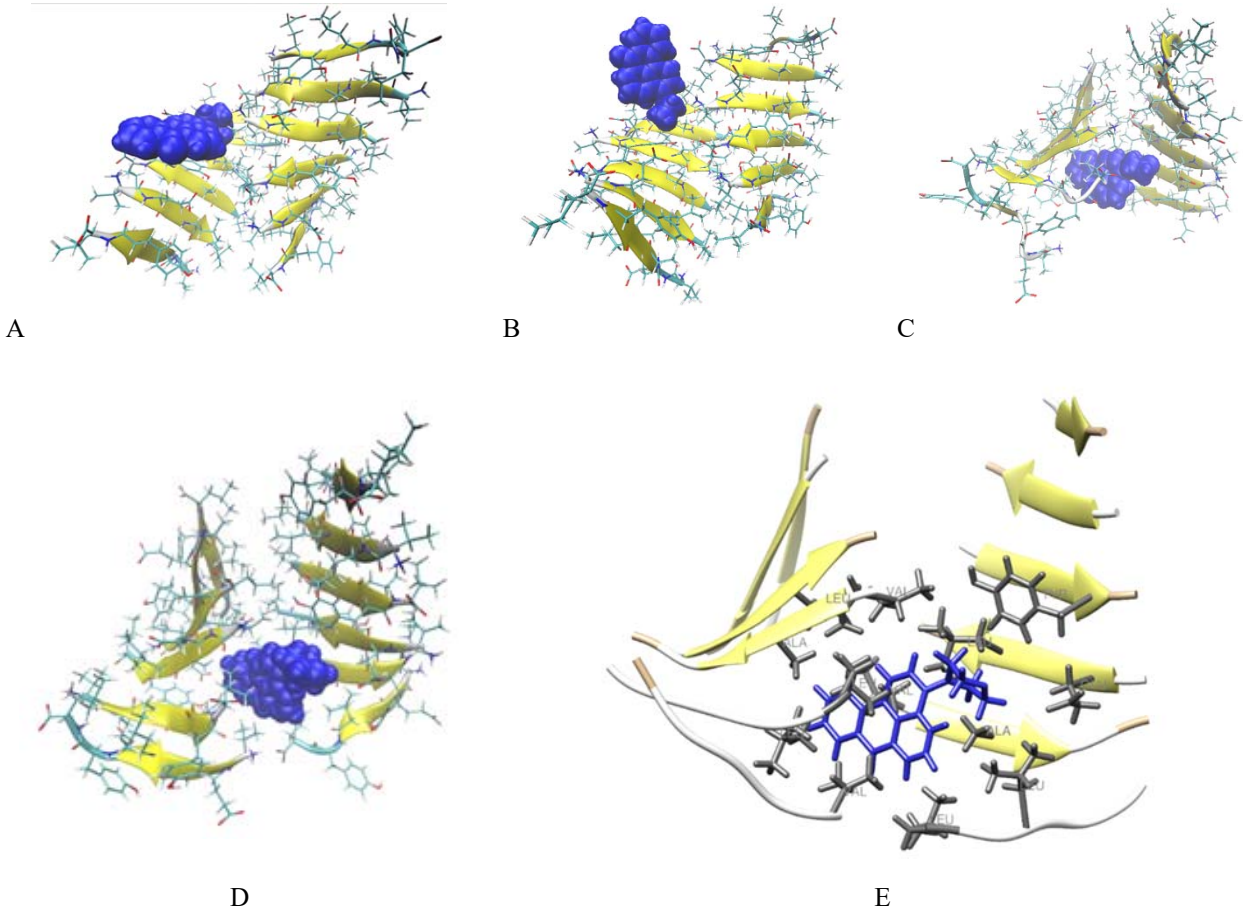

Figure 7. The snapshots of the 20 ns MD simulation of the best docking complex between ABM and vealyl (relaxed) amyloid fibril. A – 0 ns, B – 5 ns, C – 10 ns, D,E – 20 ns. The protein and ABM structures are represented as NewCartoon/Bonds and VDW/Sticks, respectively. The protein is colored according to the secondary structure: yellow – extended β-sheets, cyan/peach – β-turns, white – coil. Vealyl residues, interacting with ABM, are represented as sticks and colored in dim grey (E).

Furthermore, a deeper penetration of ABM into the dry interface between the β-sheets, as well as the increased number of LEU and VAL residues surrounding the dye after 20 ns MD simulations, as compared to that for the ABM-vealyl (relaxed) complex (Figs. 6A,7A), indicate that strong ABM-protein hydrophobic interactions are involved in the complex formation and stabilization. Interestingly, the change of the ABM binding mode may be due to the fact, that the dye molecule with the corrected charges on atoms was used for MD simulations. Notably, the dye orientation with respect to the fibril long axis significantly differed from that of ThT (Fig. 5B), suggesting the different physico-chemical determinants behind the ABM and ThT sensitivity to the amyloid structures. Indeed, ThT belongs to the class of molecular rotors and parallel orientation of the dye to the fibril axis is a necessary prerequisite for the stable ThT- fibril complex, followed by the increase of the dye planarity and significant fluorescence enhancement [23,24]. Such an orientation allows ThT to be entrapped into the fibril grooves and to form π-stacking and hydrophobic interactions with the amino acid side chains [6,23]. In contrast, ABM showed the increased quantum yield and ca. 77 nm shift of the fluorescence spectrum to the shorter wavelengths upon the dye transfer from polar ethanol to nonpolar benzene [25]. Notably, ABM (0.3 μM) binding to the insulin fibrils (12 μM) formed at pH 2, 37 °C induced the 3-fold fluorescence increase and about 70 nm blue shift of the emission maximum, as compared to that in buffer solution (Fig. 8A). Furthermore, ABM was also reported to possess high quantum yields in the presence of phospholipid membranes [22], suggesting that its sensitivity to insulin amyloid structures may result from the decrease of the environmental polarity [5]. Notably, dihedral angle between ABM benzanthrone and morpholine groups, which may rotate relative to each other, varied drastically from 0 to 150° during MD simulations, and the average torsion angle was about 90° (data not shown). Thus, unlike ThT, ABM

molecule remains non-planar in the dynamically stable dye-fibril complex, suggesting that a high fluorescence response of the dye to the insulin amyloid assemblies can hardly be explained by the decreased ABM torsion angle. Notably, our quantum-chemical calculations revealed that ABM molecular volume and width were about 12% and 40% greater, respectively, than those of ThT, and the neutral dye molecule was characterized by significantly greater lipophilicity as compared to the positively charged ThT counterpart (Table 1) [22,24,26]. These data provide additional evidence for the ability of ABM to form stronger hydrophobic and van der Waals contacts with biomolecules, as compared to that of ThT.

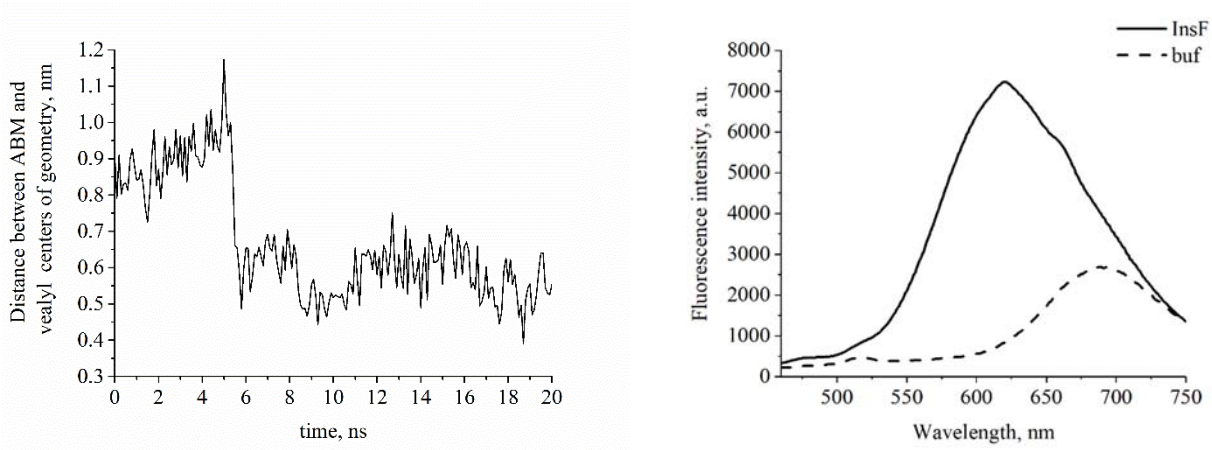

A B

Figure 8. A – Distance between ABM and vealyl (relaxed) fibril centers of geometry during MD simulation. B – Fluorescence spectra of ABM (0.3 μM) in Tris-HCl buffer (10 mM, pH 7.4) and in the presence of bovine insulin (InsF) amyloid fibrils (12 μM), formed at pH 2, 37 °C and continuous shaking for 2 days. ABM was excited at 440 nm and fluorescence spectra were recorded by Shimadzu RF-6000 spectrofluorimeter.

Table 1.

Quantum-chemical characteristics of ABM and ThT after geometry optimization*

Quantum-chemical parameter	Dye	
	ABM	ThT
Length, Å	11.8	14.3
Width, Å	7.9	5.7
Height, Å	3.4	3.7
Molecular volume, Å^3	359	318
Lipophilicity (LogP)	4.52	-0.14

*these data were reported in our previous papers

Thus, MD simulations showed that ABM lacks specificity to the insulin amyloid fibrils structures, because only the binding parallel the fibril long axis is a characteristic feature of the fluorescent amyloid markers. However, in contrast to ThT, ABM is capable of associating with the twisted amyloid assemblies.

Our previous fluorescence studies revealed that ThT had stronger association constant with the insulin amyloid fibrils (*ca.* 0.5 μM^{-1}), than ABM (*ca.* 0.2 μM^{-1}) [5]. Furthermore, Kuznetsova et al. reported ~40 times greater affinity of the ThT binding to the insulin fibrils of different morphology, revealing high specificity of the dye to the fibrillar assemblies [27]. Such disagreement between the experimental results and MD simulations can be explained by the fact that crystal structures of the insulin fibrillar fragments obtained by X-ray structural analysis, are flattened, allowing the formation of the specific fibril binding sites for the dyes with high affinity [13]. In turn, the vealyl (relaxed) fibril is twisted, so the stable ThT complexes with the vealyl fibril may be obtained if the non-relaxed (flattened) vealyl structure is used in MD simulations in combination with weak position restraints applied to the protein atoms (that should prevent twisting of the fibril).

The backbone $RMSD$ value for the free vealyl (relaxed) fibril, as well as for the ABM-vealyl (relaxed) complex, did not increase significantly during the MD simulation, and attained equilibrium value ~0.25 nm in ~10 ns, suggesting the dynamic stability of the protein structure in the last 10 ns of the simulation (Fig. 9A). It should be noted that the fibril compactness remained unchanged for 20 ns of the simulation, because the R_g value was ~1.3 nm for both the free vealyl (relaxed) and its complex with ABM (Fig. 9B). Thus, the ABM molecule did not induce noticeable alterations in the fibril structure, and the dye binding mode to the vealyl (relaxed) revealed by the MD simulation should be reliable due to the dynamic stability of the fibrillar assembly.

To further characterize the ABM binding to the vealyl (relaxed) fibril, we calculated the binding free energy $\left(\Delta G_{binding}\right)$ and its components by analyzing the MD trajectory obtained for the most stable ABM-vealyl (relaxed) docked complex

(Fig. 10) using the GMXPBSA GROMACS tool. The $\Delta G_{binding}$ value was equal to –31.4±1.8 kJ/mol, that is in good agreement with the results obtained for ABM association with bovine insulin amyloid fibrils at 25°C, pH 7.4 $\left(\Delta G_{binding} = -30.2 \text{ kJ/mol}\right)$ [5]. Furthermore, the Lennard-Jones component showing the strongest favorable contribution was increased, while the Coulombic and nonpolar solvation terms showing the weak favorable contributions remained unchanged during the 20 ns MD simulation, and the polar solvation term that strongly unfavored the ABM-vealyl complex formation was decreased (Fig. 10A).

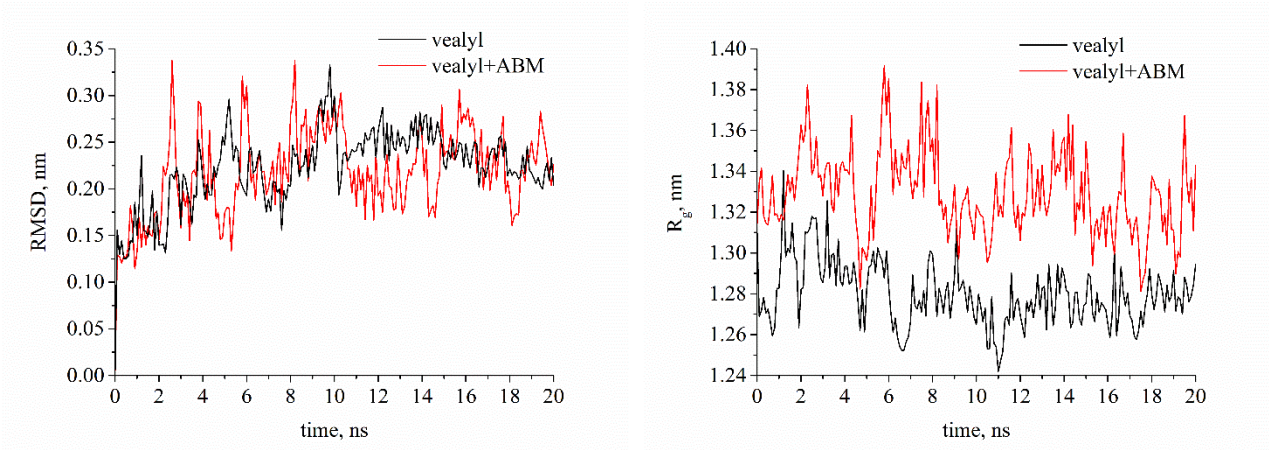

A B

Figure 9. A – Time evolution of vealyl (relaxed) fibril *RMSD* (backbone) (A) and radius of gyration (R_g) (B) at 310.15 K during MD simulation in the absence and in the presence of ABM.

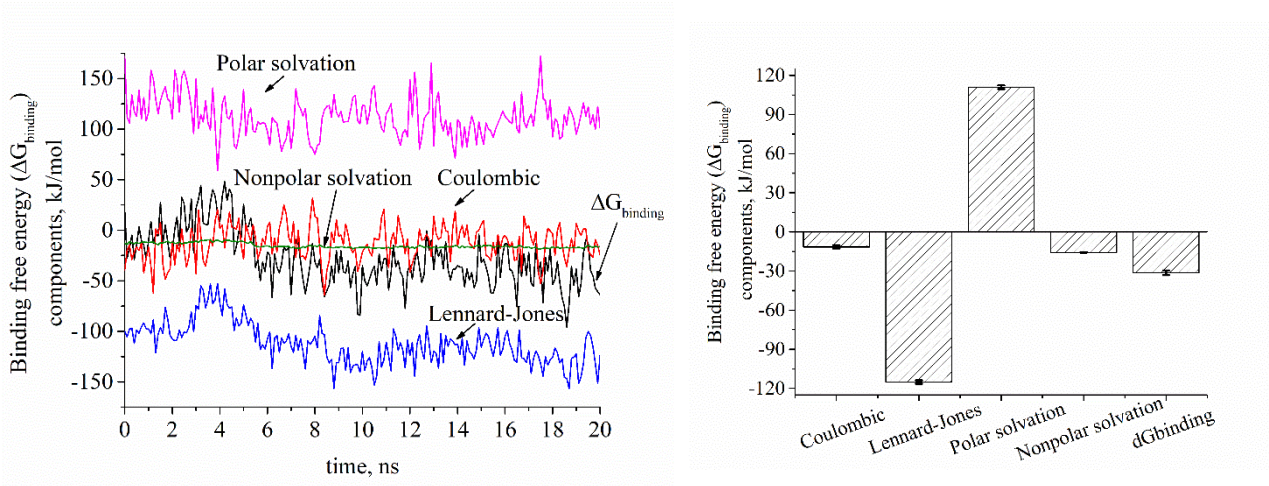

A B

Figure 10. A – Free energy terms for the ABM-vealyl fibril (relaxed in water) during MD simulation, determined using the GMXPBSA program (v 2.1.2), the Gromacs tool for calculating the binding free energies of a protein-ligand complex by MM/PBSA method [10]. $\Delta G_{binding}$ – binding free energy. Nonpolar solvation energy component is reduced during the simulation, and the Lennard-Jones energy is increased (by module). $\Delta G_{binding}$ calculations were performed at 310.15 K, 0.15 M NaCl, using the protein dielectric constant of *ca.* 2, cutoff-scheme Verlet and constraints for H-bonds. The Coulombic energy terms were calculated in Gromacs 2020.2. The polar and nonpolar solvation energy values were determined using the APBS suite 1.4.1. B – Final values of the ABM- fibril (relaxed in water) binding energy and its components, averaged over 20 ns MD trajectory.

The obtained energy contributions are the quantitative characteristics of the processes occurring during the MD simulations: i) the decrease of ABM-vealyl distance (Fig.8A), indicating the strengthening of the van der Waals dye-protein interactions; ii) ABM penetration in the dry interface between the two β-sheets, resulting in the weakening of destabilizing dye-solvent interactions; iii) reduced number of GLU residues in close vicinity of the uncharged dye, leading to the decrease of the unfavorable dye-protein electrostatic interactions. The values of $\Delta G_{binding}$ and its constituents are presented in Fig. 10B and Table 2.

Interestingly, the obtained overall $\Delta G_{binding}$ value was about 3.5 times lower than that for the binding of the Morin hydrate to the native insulin molecule [28], similar to that reported for the Tacrine, flavonoid quercetin hybride inhibitor

of Aβ pathogenic aggregation [29], and about 2.5 times greater than that for ThT complexation with the amyloid-β(1−42) fibril [18], revealed by GMXPBSA. Remarkably, in the latter study ThT was located on the dry steric zipper interface between the two β-sheets of the amyloid-β(1−42) fibrillar assembly, and associated with the groove formed by LEU and PHE residues.

Table 2.

Free energy of ABM binding to vealyl (relaxed) fibril averaged over 20 ns MD trajectory, calculated by GMXPBSA GROMACS tool

Binding free energy terms	$\Delta G_{binding}$, kJ/mol
Coulombic (E_{coul})	–11.5±1.3
Lennard-Jones (E_{LJ})	–115.1±1.4
Polar solvation (G_{polar})	111.0±1.5
Nonpolar solvation ($G_{nonpolar}$)	–15.8±0.2
Polar contribution ($G_{polar} + E_{coul}$)	99.5
Non-polar contribution ($G_{nonpolar} + E_{LJ}$)	–130.8
Binding free energy ($\Delta G_{binding}$)	–31.4±1.8
Binding free energy revealed by fluorescence studies ($\Delta G_{binding}^{experimental}$)*	–30.2

* ABM association constant (K_a) with insulin fibrils at pH 7.4, 25 °C determined previously from the fluorescence studies is equal to 0.2 μM^{-1} ($\Delta G_{binding}^{experimental} = -RT \ln K_a$) [5]

CONCLUSIONS

In conclusion, the molecular docking and molecular dynamics simulations studies revealed two typical binding modes of the benzanthrone dye ABM and the standard amyloid marker Thioflavin T to the model insulin amyloid fibrils, i.e. the binding to the β-sheet surface and to the β-sheet edges. The former was predominant for both dyes, forming hydrophobic and van der Waals contacts with the neutral amino acids LEU, VAL, TYR, ALA, ASN and GLN, although ABM and ThT were oriented perpendicular and parallel to the fibril long axis, respectively. The binding free energy of ABM to the fibrillar insulin was similar to that derived from the fluorescence studies. The Lennard-Jones, Coulombic and nonpolar solvation terms contributed positively to the overall binding free energy, revealing that high affinity of the ABM molecule to the amyloid fibrils results from the dye binding to the hydrophobic interface between the insulin β-sheets. Overall, the ABM sensitivity to the environmental polarity is likely to be the key factor in the dye fluorescence response to the presence of insulin fibrillar assemblies. Further studies should be carried out for the insulin fibrillar structures with the enhanced dynamic stability, in order to keep the protein binding sites for the small ligands intact during the MD simulation and thus, to provide greater accuracy for the atomistic mechanism of the dye-protein interactions, that is important for sensible design of the novel amyloid markers and anti-amyloid agents.

ACKNOWLEDGEMENTS

This work was supported by the Ministry of Education and Science of Ukraine (the Young Scientist projects № 0117U004966 "Nano- and microsized liophylic and liophylized self-associated systems: application in modern technologies and biomedicine" and the project № 0119U002525 "Development of novel ultrasonic and fluorescence techniques for medical micro- and macrodiagnostics"). The author is grateful to Dr.Sci. Galyna Gorbenko, V. N. Karazin Kharkiv National University, for useful comments and discussions.

ORCID IDs

Kateryna Vus, http://orcid.org/0000-0003-4738-4016

REFERENCES

[1] L. Tran, and T. Ha-Duong, Peptides. **69**, 86-91 (2015), https://doi.org/10.1016/j.peptides.2015.04.009.
[2] W.M. Berhanu, and A.E. Masunov, J. Mol. Model. **18**, 1129-1142 (2012), https://doi.org/10.1007/s00894-011-1123-3.
[3] M. Biancalana, and S. Koide, Biochim. Biophys. Acta. **1804**, 1405-1412 (2010), https://doi.org/10.1016/j.bbapap.2010.04.001.
[4] C. Wu, J. Scott, and J.E. Shea, Biophys. J. **103**, 550-557 (2012), https://doi.org/10.1016/j.bpj.2012.07.008.
[5] K.O. Vus, *Fluorescence detection of amyloid fibrils, PhD Thesis:* 03.00.02. Kharkiv, 2016, P. 94, http://rbecs.karazin.ua/wp-content/uploads/2015/dis/dis_Vus.pdf.
[6] M.R. Krebs, E.H. Bromley, and A.M. Donald, J. Struct. Biol. **149**, 30-37 (2005), https://doi.org/10.1016/j.jsb.2004.08.002.

[7] E. Vanquelef, S. Simon, G. Marquant, E. Garcia, G. Klimerak, J.C. Delepine, P. Cieplak, and F.Y. Dupradeau, Nucleic Acids Res. **39**, W511-W517 (2011), https://doi.org/10.1093/nar/gkr288.
[8] A. Grosdidier, V. Zoete, and O. Michielin, Nucleic Acids Res. **39**, W270-W277 (2011), https://doi.org/10.1093/nar/gkr366.
[9] A. Grosdidier, V. Zoete, and O. Michielin, J. Computational Chem. **32**, 2149-2159 (2011), https://doi.org/10.1002/jcc.21797.
[10] C. Paissoni, D. Spiliotopoulos, G. Musco, and A. Spitaleri, Computer Physics Communications. **186**, 105-107 (2015), https://doi.org/10.1016/j.cpc.2014.09.010.
[11] I. Massova, and P.A. Kollman, J. Am. Chem. Soc. **121**, 8133-8143 (1999), https://doi.org/10.1021/ja990935j.
[12] UCLA-DOE Institute, 611 Young Drive East, Los Angeles, CA 90095, https://people.mbi.ucla.edu/sawaya/jmol.
[13] M.R. Sawaya, S. Sambashivan, R. Nelson R, M.I. Ivanova, S.A. Sievers, M.I. Apostol, M.J. Thompson, M. Balbirnie, J.J.W. Wiltzius, H.T. McFarlane, A.O. Madsen, C. Riekel, and D.Eisenberg, Nature, **447**, 453-457 (2007), https://doi.org/10.1038/nature05695.
[14] M.I. Ivanova, S.A. Sievers, M.R. Sawaya, J.S. Wall, and D. Eisenberg, PNAS. 106, 18990-18995 (2009), https://doi.org/10.1073/pnas.0910080106.
[15] N Amdursky, M.H. Rashid, M.M. Stevens, and I. Yarovsky, Sci. Rep. **7**, 6245 (2017), https://doi.org/10.1038/s41598-017-06030-4.
[16] C.J. Stein, J.M. Herbert, and M. Head-Gordon, J. Chem. Phys. **151**, 224111 (2019), https://doi.org/10.1063/1.5131020.
[17] J. Dzubiella, J.M.J. Swanson and J.A. McCammon, J. Chem. Phys. **124**, 084905 (2006), https://doi.org/10.1063/1.2171192.
[18] G. Kuang, N.A. Murugan, Y. Tu, A. Nordberg, and H. Ågren, J. Phys. Chem. B, **119**, 11560-11567 (2015), https://doi.org/10.1021/acs.jpcb.5b05964.
[19] V. Trusova, East European Journal of Physics. **2**, 51-58 (2015), https://doi.org/10.26565/2312-4334-2015-2-06.
[20] A. Kokorev, V. Trusova, K. Vus, U. Tarabara, and G. Gorbenko, East European Journal of Physics. **4**, 30-36 (2017), https://doi.org/10.26565/2312-4334-2017-4-04.
[21] G. Gorbenko, V. Trusova, E. Kirilova, G. Kirilov, I. Kalnina, A. Vasilev, S. Kaloyanova, and T. Deligeorgiev, Chem. Phys. Lett. **495**, 275-279 (2010), https://doi.org/10.1016/j.cplett.2010.07.005.
[22] O. Ryzhova, K. Vus, V. Trusova, E. Kirilova, G. Kirilov, G. Gorbenko ,and P. Kinnunen, Methods Appl. Fluoresc. **4**, 034007 (2016), https://doi.org/10.1088/2050-6120/4/3/034007.
[23] M. Biancalana, K. Makabe, A. Koide and S. Koide, J. Mol. Biol. **385**,1052-1063 (2009), https://doi.org/10.1016/j.jmb.2008.11.006.
[24] V.I. Stsiapura, A.A. Maskevich, V.A. Kuzmitsky, K.K. Turoverov, and I.M. Kuznetsova, J. Phys. Chem. A. **111**, 4829-4835 (2007), https://doi.org/10.1021/jp070590o.
[25] E.M. Kirilova, I. Kalnina, G.K. Kirilov and I. Meirovics, J. Fluoresc. **18**, 645-648 (2008), https://doi.org/10.1007/s10895-008-0340-3.
[26] U. Tarabara, M. Shchuka, K. Vus, O. Zhytniakivska, V. Trusova, G. Gorbenko, N. Gadjev, and T. Deligeorgiev, East European Journal of Physics. **4**, 58-69 (2019), https://doi.org/10.26565/2312-4334-2019-4-06.
[27] I.M. Kuznetsova, A.I. Sulatskaya, V.N. Uversky, and K.K. Turoverov, PloS ONE. **7**, e30724 (2012), https://doi.org/10.1371/journal.pone.0030724.
[28] P. Patel, K. Parmar, and M. Das, Int. J. Biol. Macromol. **108**, 225-239 (2018), https://doi.org/10.1016/j.ijbiomac.2017.11.168.
[29] R.H. Gharacheh, M. Eslami, P. Amani, and S.B. Novir, Phys. Chem. Res. **7**, 561-579 (2019), https://doi.org/10.22036/PCR.2019.183077.1624.

ДОСЛІДЖЕННЯ ЗВ'ЯЗУВАННЯ БЕНЗАНТРОНОВОГО ЗОНДА АБМ З АМІЛОЇДНИМИ ФІБРИЛАМИ ІНСУЛІНУ МЕТОДАМИ МОЛЕКУЛЯРНОГО ДОКІНГУ ТА МОЛЕКУЛЯРНО-ДИНАМІЧНОГО МОДЕЛЮВАННЯ

К. Вус
Кафедра медичної фізики та біомедичних нанотехнологій, Харківський національний університет імені В.Н. Каразіна
м. Свободи 4, Харків, 61022, Україна

За допомогою молекулярного докінгу та молекулярно-динамічного моделювання (MD) досліджено зв'язування бензантронового зонда АВМ з амілоїдними фібрилами інсуліну людини, які позначено тут як vealyl, lyqlen та Insf, що складалися із амінокислотних залишків 12-VEALYL-17 (B-ланцюг інсуліну), 13-LYQLEN-18 (A-ланцюг інсуліну), 11-LVEALYL-17 (B-ланцюг інсуліну) + 12-SLYQLENY-19 (A-ланцюг інсуліну), відповідно. На першому етапі роботи амілоїдні структури інсуліну було сольватовано та проведено MD еквілібрацію при температурах 300–310 K (у пакеті ГРОМАКС) з використанням позиційних обмежень руху атомів білкового остова, для попередження руйнування β-листів. Виявлено, що релаксація фібрил vealyl призвела до закручення двох β-листів відносно довгої осі фібрили, причому тільки цей тип фібрил залишився стабільним упродовж 20 нс MD-симуляції релаксованих структур. На наступному етапі роботи, фібрили Insf, vealyl, lyqlen, та vealyl (релаксована) було використано для молекулярного докінгу (за допомогою SwissDock), що дозволило визначити типи сайтів зв'язування АВМ та стандартного амілоїдного маркеру тіофлавіну T (ThT) з досліджуваними амілоїдними структурами. Зокрема, у найбільш енергетично вигідному комплексі фібрили vealyl (релаксована) сайт зв'язування для АВМ був розташований на гідрофобній поверхні одного з двох β-листів. MD-симуляція протягом 20 нс призвела до зміни положення АВМ на фібрилі інсуліну – зонд став глибше зануреним у гідрофобну область між двома β-листами, що супроводжувалося взаємодією з такими амінокислотними залишками: 6 LEU, 3 VAL, 2 ALA, 1 TYR та 1 GLU. Значення вільної енергії зв'язування ($\Delta G_{binding}$) АВМ з фібрилою vealyl (релаксована), що отримано за допомогою GROMACS інструменту GMXPBSA, складало –31.4±1.8 кДж/моль, що узгоджується з оцінкою, отриманою за допомогою флуоресцентних досліджень асоціації АВМ з амілоїдними фібрилами інсуліну при температурі 25°C, pH 7.4 ($\Delta G_{binding}$= - 30.2 кДж/моль). Компонента Леннарда-Джонса домінувала у взаємодії між зондом та фібрилою, кулонівський компонент та компонент неполярної сольватації мали слабкі вклади у сумарне значення $\Delta G_{binding}$, а компонент полярної сольватації мав несприятливий ефект на формування комплексу між АВМ та фібрилою vealyl (релаксована). Отримані результати свідчать про те, що значна специфічність АВМ до амілоїдних фібрил інсуліну, спостерігається, переважно, завдяки сильним гідрофобним взаємодіям між зондом та білком, що супроводжується формуванням підвищеної кількості ван-дер-

Ваальсових зв'язків, і також додатково підтверджує спостережувану раніше чутливість спектральних властивостей ABM до полярності оточення. Таким чином, отримані результати дають більш детальну картину зв'язування бензантронового зонда ABM з амілоїдними фібрилами інсуліну на атомному рівні, та можуть бути використані у розробці нових флуоресцентних репортерів, що мають високу специфічність до амілоїдних ансамблів інсуліну.
КЛЮЧОВІ СЛОВА: АБМ, амілоїдні фібрили інсуліну, вільна енергія зв'язування, молекулярний докінг, молекулярно-динамічне моделювання, тіофлавін Т.

ИЗУЧЕНИЕ СВЯЗЫВАНИЯ БЕНЗАНТРОНОВОГО ЗОНДА АБМ С АМИЛОИДНЫМИ ФИБРИЛЛАМИ ИНСУЛИНА МЕТОДАМИ МОЛЕКУЛЯРНОГО ДОКИНГА И МОЛЕКУЛЯРНО-ДИНАМИЧЕСКОГО МОДЕЛИРОВАНИЯ

К. Вус
Кафедра медицинской физики и биомедицинских нанотехнологий
Харьковский национальный университет имени В.Н. Каразина
пл. Свободы 4, Харьков, 61022, Украина

При помощи молекулярного докинга и молекулярно-динамического моделирования (MD) исследовано связывание бензантронового зонда ABM с амилоидными фибриллами инсулина человека, обозначенными здесь как vealyl, lyqlen и Insf, которые состояли из аминокислотных остатков 12-VEALYL-17 (B-цепь инсулина), 13-LYQLEN-18 (A-цепь инсулина), 11-LVEALYL-17 (B-цепь инсулина) + 12-SLYQLENY-19 (A-цепь инсулина), соответственно. На первом этапе работы амилоидные структуры инсулина были сольватированы и была проведена MD-эквилибрация при температурах 300–310 K (в пакете ГРОМАКС) с применением позиционных ограничений движения атомов белкового остова, для предотвращения разрушения β-листов. Обнаружено, релаксация фибрилл vealyl привела к закручиванию двух β-листов относительно длинной оси фибриллы, причем только этот тип фибрилл оставался стабильным в течение 20 нс MD-симуляции релаксированных структур. На следующем этапе работы, фибриллы Insf, vealyl, lyqlen, и vealyl (релаксированная) были использованы для молекулярного докинга (при помощи SwissDock), что позволило определить типы сайтов связывания ABM и стандартного амилоидного маркера тиофлавина T (ThT) с исследуемыми амилоидными структурами. В частности, в наиболее энергетически выгодном комплексе фибриллы vealyl (релаксированная) сайт связывания для ABM был расположен на гидрофобной поверхности одного из двух β-листов. MD-симуляция в течение 20 нс привела к изменению положения ABM на фибрилле инсулина – зонд глубже погрузился в гидрофобную область между двумя β-листами, что сопровождалось взаимодействием с такими аминокислотными остатками: 6 LEU, 3 VAL, 2 ALA, 1 TYR и 1 GLU. Значения свободной энергии связывания ($\Delta G_{binding}$) ABM с фибриллой vealyl (релаксированная), полученное при помощи GROMACS инструмента GMXPBSA, составило –31.4±1.8 кДж/моль, что согласуется с оценкой, полученной при помощи флуоресцентных исследований ассоциации ABM с амилоидными фибриллами инсулина при температуре 25 °C, pH 7.4 ($\Delta G_{binding}$= - 30.2 кДж/моль). Компонента Леннарда-Джонса доминировала во взаимодействии между зондом и фибриллой, кулоновская компонента и компонента неполярной сольватации имели слабые вклады в суммарное значение $\Delta G_{binding}$, а компонента полярной сольватации имела неблагоприятное влияние на образование комплекса между ABM и фибриллой vealyl (релаксированная). Полученные результаты свидетельствуют о том, что значительная специфичность ABM к амилоидным фибриллам инсулина, наблюдается, преимущественно, благодаря сильным гидрофобным взаимодействиям между зондом и белком, сопровождаемым формированием повешенного числа ван-дер-Ваальсовых контактов, что также дополнительно подтверждает наблюдаемую ранее чувствительность спектральных свойств ABM к полярности окружения. Таким образом, полученные результаты дают более детальную картину связывания бензантронового зонда ABM с амилоидными фибриллами инсулина на атомном уровне, и могут быть использованы при разработке новых флуоресцентных репортеров, которые имеют высокую специфичность к амилоидным ансамблям инсулина.
КЛЮЧЕВЫЕ СЛОВА: АБМ, амилоидные фибриллы инсулина, свободная энергия связывания, молекулярный докинг, молекулярно-динамическое моделирование, тиофлавин Т.